Forced and Free Variations of the Surface Temperature Field in a General Circulation Model

GERALD R. NORTH, KUOR-JIER JOSEPH YIP, AND LAI-YUNG LEUNG

Climate System Research Program, Department of Meteorology, Texas A&M University, College Station, Texas

ROBERT M. CHERVIN

National Center for Atmospheric Research, Boulder, Colorado

(Manuscript received 16 November 1990, in final form 1 July 1991)

ABSTRACT

The concept of "forced" and "free" variations of large-scale surface temperature is examined by analyzing several long runs of the Community Climate Model (CCM0) with idealized boundary conditions and forcing. 1) The planet is all land with uniform sea-level topography and fixed soil moisture. 2) The planetary surface and prescribed ozone are reflection symmetric across the equator and there is no generation of snow. 3) The obliquity is set to zero so that the climate is for a perpetual equinox solar insolation (i.e., sun fixed over the equator). After examining some relevant aspects of the undisturbed climate (surface temperature field) such as temporal and spatial autocorrelations and the corresponding spectra, two types of changes in external forcing are imposed to study the model response: 1) sinusoidal changes of the solar constant (5%, 10%, 20%, and 40% amplitudes) at periods of 15 and 30 days (the latter is the autocorrelation time for the global average surface temperature) and 20% at 60 days and 2) insertion of steady heat sources (points and zonal bands) of variable strength at the surface. Then the temporal spectra of large scales for the periodically forced climate and the ensemble-averaged influence functions are examined for the point source disturbed climates. In each class of experiments the response of ensemble-averaged amplitudes was found to be proportional to the amplitude of the forcing. These results suggest that the lowest moments of the surface temperature field have a particularly simple dependence on forcing. Furthermore, the apparent finiteness of the variance spectrum at low frequencies suggests that estimates of long-term statistics are stable in this type of atmospheric general circulation model.

1. Introduction

More than a decade ago Saltzman (1978) and later Lorenz (1979) introduced the nomenclature "forced" and "free" in referring to fluctuations of a field in the climate system. Lorenz studied geopotential height data from a ten-year dataset taken from the real atmosphere. He concluded that the seasonal cycle on the largest scales might be considered "forced" while variations at other frequencies and scales seemed to be "free" in the sense that they do not appear to be deterministic in the statistical sense. In this paper we carry the study further by examining some long runs of a widely used general circulation model (GCM).

Among the many puzzles associated with climate modeling is the role of nonlinearity in the governing equations. "Pessimists" have argued that the climate system is so complex and nonlinear that reliable results can never be expected to come from numerical simulations. Perhaps the most perplexing nonlinearity to affect climate is that due to the advection term in the Navier-Stokes equations. This important term leads to various flow instabilities and even to turbulence under certain conditions. In terms of local climate, temperature-changing heat is brought into a region by advecting winds, but the very circulation of the winds is a nonlinear functional of the background temperature field, which in turn is determined by heat advection as well as other energy fluxes. In this study we explore the possibility that the advection effects can be considered at least statistically as a linear functional of the surface temperature for the purposes of computing the response of the surface temperature field to relatively slowly changing conditions. The linear response hypothesis is not intuitively appealing at first glance, since local day-to-day temperature fluctuations are dominated by advection. Stone (1978) has argued for a nonlinear form of the diffusion process.

The linearity hypothesis is an extremely difficult one to test with real data. Lorenz's (1979) attempt with 500-mb heights reached the conclusion that some of the large-scale forced responses (seasonal) were linear, but much of the variance could not be attributable to linear responses. He conjectured that a random forcing

Corresponding author address: Dr. Gerald R. North, Texas A&M University, Climate System Research Program, College Station, TX 77843-3150.

term might be useful in generating the so-called "free" atmospheric fluctuations. Our approach is to generate an artificial climate with a commonly used general circulation model of the atmosphere instead of using data collected from stations on the real earth. Of course, this approach is only as good as the model, and there is considerable controversy about the validity of such models. However, we adopt the philosophy that currently used models themselves are worthy of study, and the advantages they offer in terms of controllability of experimental conditions are compelling. Still one must be cautious in applying our conclusions to the real earth's climate.

In this paper, we report the results of a series of basic experiments conducted with a modified version of the original NCAR Community Climate Model (CCM0: circulation statistics and documentation can be found in Washington 1982; Pitcher et al. 1983; Ramanathan et al. 1983; Malone et al. 1984; Chervin 1986). Our findings indicate that in the absence of certain obvious nonlinearities, such as snow-albedo feedback, the ensemble-averaged surface thermal field behaves in an essentially linear manner. In order to conduct our experiments we idealized the boundary conditions as follows: 1) The planetary surface was made to be all land. 2) All topographic features such as mountains were removed to make a zonally symmetric lower boundary at sea level. 3) The obliquity (tilt angle of the planetary spin axis with respect to a normal to the orbital plane) of the planet was set to zero so that it ran in an equinox solar insolation regime perpetually. 4) The surface albedo and ozone distributions were prescribed as zonally symmetric, reflection symmetric about the equator, and fixed in time (no snow-albedo feedback). In this version of the model, the land surface temperature is determined by an iterative solution to a heat balance equation assuming no net heat conduction across the interface. This heat balance equation does not permit any heat storage in the ground, and hence no long timescale forcing is possible from subsurface storage and release of heat. Furthermore, the surface hydrology is noninteractive as soil moisture is not a predicted variable.

The purpose of the above simplifications was to effectively lengthen any time series generated by removing the longer time constant associated with a mixed-layer ocean (resulting in a factor of 60 effective increase in the time series; by effective we mean in units of the autocorrelation time), making every longitude statistically equivalent (further allowing the pooling of data), making the planet statistically symmetric across the equator (resulting in another factor of 2 in time series length), and by removing the seasonal cycle naturally rendering the time series stationary (resulting in another effective lengthening of the time series). For many purposes the time series is lengthened by these measures by a factor of 1000 over the conventional simulations including geography and seasons. Even though these simplifications make our interpretation of the results easier and result in a considerable economy of computing time, we have not sacrificed physical realizability in the sense that we could imagine a real planet with these properties. We emphasize that no mutilation has occurred in the implementation of the physical laws or in the numerical procedures (beyond those committed in the creation of the original CCM0)—we are simply studying a planet that is different from earth but bearing some interesting similarities. At the same time, we must keep in mind that some important features of the planet earth are connected with the very asymmetry features we are omitting.

Our goal is to understand the surface thermal climate of this simplified planet, termed *Terra Blanda,* by making long undisturbed runs on the Texas A&M Cray YMP single processor supercomputer (a 15-year simulation requires about 75 hours of computer time) and by making perturbations in the forcing and studying the response of the surface temperature field. In this paper we report only the properties of the surface temperature field, but we intend to study other fields in subsequent investigations. Our choice of the surface temperature field is driven in part by our long experience with energy-balance climate models (EBMs), which treat only the surface temperature field (e.g., North et al. 1981; and most recently Hyde et al. 1989). These EBM studies have shown that the radiation budget at the top of the atmosphere is mainly responsible for the surface thermal distribution, and apparently many of the smoothing effects of total horizontal heat transport may be modeled as a linear downgradient diffusion process. This simplification is not likely to hold for many fields other than the ensemble-averaged surface temperature field in the atmospheric or oceanic system. That such a linear model was able to fit the observed geographical distribution of the annual and semiannual harmonics of the seasonal cycle of the surface temperature field already constituted strong evidence of linearity in this field to periodic forcing at the annual and semiannual frequencies (North et al. 1983a). Furthermore, the same EBM was able to match the CCM0 as boundary conditions were altered according to paleoclimate data back to 18 000 years BP (Hyde et al. 1989). Still one was left with an uneasy feeling that the matches might have been achieved by coincidence and certainly without the control that could be achieved through direct experimentation with the CCM0 treated as a "black box."

Before proceeding, it is good to recall that the CCM0 is a highly simplified representation of an earthlike atmosphere. It is basically a nine-layer spectral model with rhomboidal truncation at degree 15 (R15). This translates to a latitude–longitude grid of approximately $4.5° \times 7.5°$. Furthermore, the convective schemes used in the model are simplified compared to the next version of the model (e.g., cf. Hoerling et al. 1990; Randel

and Williamson 1990). We hope to repeat some of our experiments with later versions of the CCM and possibly other GCMs as appropriate in the future. We always run the risk that the CCM0 (and any other current generation GCM) is more like an EBM in its surface temperature field than it is like nature. The model does include cloud and water vapor feedbacks.

The plan of the paper is to first present some relevant statistical properties of the undisturbed climate [various other aspects of the undisturbed climate can be found in a separate paper by Leung and North (1991)] and then introduce the perturbations in the following section, after which we summarize and draw conclusions.

2. Surface climate of *Terra Blanda*

Some interesting aspects of the surface climate of the planet are discussed in more detail elsewhere (Leung and North 1991) so that only certain relevant results are reported here. In that paper, considerable attention is directed to objectively fitting the parameters of a noise-forced EBM to the CCM0-generated undisturbed climate. That effort proved successful in that the EBM free parameters (effective land surface heat capacity density, C, and the thermal diffusion coefficient, D; these are equivalent to specifying the length and time scales of the EBM) were both found to be numerically close to those found in earlier EBM studies forced to fit the geographical distribution of the annual cycle for earth (North and Coakley 1979; North et al. 1983a; Hyde et al. 1989). The noise used to force the system was white in time and statistically homogeneous on the sphere but, perhaps surprisingly, it was "blue"

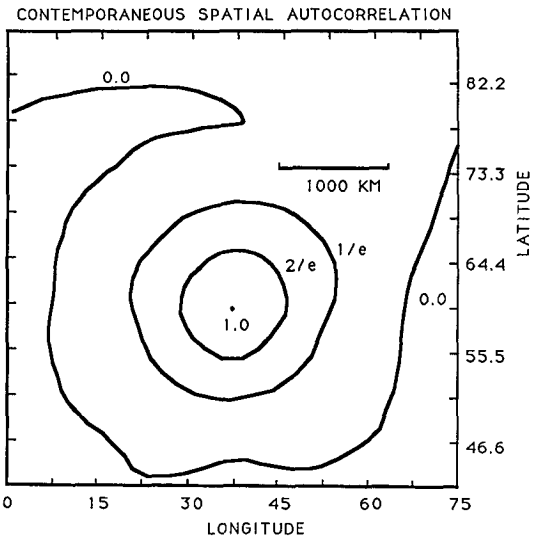

FIG. 1. Contemporaneous autocorrelation of the surface temperature with neighboring points for the undisturbed climate of *Terra Blanda* based upon a 15-year run. The control point is at 60° latitude. The horizontal and vertical scales have been adjusted so that equal physical distances correspond to equal intervals on the map.

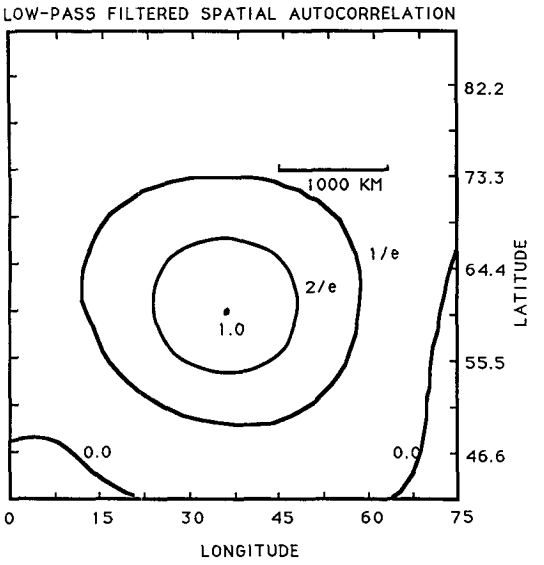

FIG. 2. Same as Fig. 1, except that the time series was low-pass filtered with a 60-day tapered moving average.

in space, being of the form of a divergence of a vector spatial white noise up to spherical harmonic degree 14 or so, after which the spectrum of forcing noise turns over ("reddens"). This last is consistent with the forcing noise being due mainly to divergences of horizontal heat and momentum fluxes on the sphere (divergence of a spatial white noise vector is spatial blue noise scalar).

Figure 1 shows the contemporaneous surface temperature correlation for points in the neighborhood of the test point located at 60° latitude. Note that the pattern is remarkably isotropic and that it exhibits a length scale of about 1300 km. In this and the next figures, the horizontal and vertical scales have been altered so that equal physical distances correspond to equal intervals along each axis. In effect, circles on the sphere should look like circles here. In Fig. 2, the same kind of illustration is seen, but the time series has now been low-pass filtered (60-day moving average) so that only low frequencies are present in the data. This is effectively the low-frequency limit, since the longest time scale in this model is about 30 days. This last comes from the fact that the globally averaged temperature is reasonably well represented by a first-order autoregressive process with autocorrelation time 30 days (Leung and North 1990, 1991); in the noise-forced EBM this time constant is just the ratio C/B (cf. North and Cahalan 1982; North et al. 1983a; Hyde et al. 1989). Note that the length scale is longer and more elongated east–west for the low-frequency case. The latter effect is due to a small eastward advection. The advection is illustrated in Fig. 3 as a contour map of spatial correlations lagged by 24 h (cf. Cahalan et al. 1982). The speed of the advection is about 2.5 m s^{-1} at this latitude and the decay of the correlations is quite

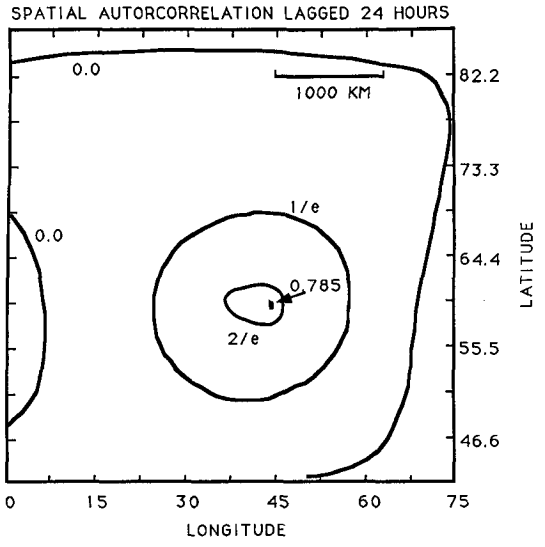

FIG. 3. Same as Fig. 1, except that the neighboring points are correlated with the test point 24 h later. The advection of the correlation cluster is clear. Note the decay of the maximum correlation over this interval.

rapid with an e-folding time of about 2.8 days. Although clearly revealed in these data and especially in the spherical spectral analysis (Leung and North 1991), the advection term is not very important for the longer time scales in most of what follows.

It is interesting that these correlations fall off with a length scale of 1000–2000 km as suggested for the EBM (North 1984; and given by the length scale $l \sim (D/B)^{1/2}$). This length scale is controlled by the diffusion parameter and the radiation damping. It may be interpreted as the distance a random walking anomaly can advance in one radiative relaxation time. Hansen and Lebedeff (1987) found a similar length scale in the middle and polar latitudes. Their correlations were computed from annual averages and were for station pairs with 50 or more years of contemporaneous (calendar year average) reports. Their graphs indicate a length scale of about 1700 km in the middle and polar latitudes with an insensitivity to latitude. Since the data were annually averaged, they were neither contemporaneous nor low-frequency limited as in our illustrations from the CCM0 data. Since the mixed layer of the real ocean has a time constant of about 5 years, they are somewhere in between the two extremes. Kim and North (1991) have used 40 years of surface data to examine the geographical dependence of the correlation length for several frequency bands. They compared their results to those found in a noise-forced EBM with full land–sea geography. For higher frequencies [$>1/(5$ yr)] the correlation lengths were found to be shorter over ocean regions than over land. For lower frequencies the correlation lengths tend to uniformize to something like 1500 km. We believe that the correlation lengths found in the CCM0 simulations of *Terra Blanda* are the same as those found in the 40 years of real earth data and in the noise-forced EBM. Another candidate for explaining such a length scale is the Rossby radius of deformation, which has the same order of magnitude. We conjecture that the radiation-damped diffusion length is the better choice since it would be hard to explain the geographical dependence of the Rossby radius 1) in going from land to ocean surfaces for higher frequencies (factor of 2, Kim and North 1991), 2) in going from polar to midlatitudes (virtually no dependence in the data, EBM, or CCM0; whereas the Rossby radius should have a dependence on latitude, since for shallow water models it is inversely proportional to the Coriolis parameter, f. We reiterate that our contention is conjectural and warrants further investigation.

No statistically significant teleconnections (e.g., Wallace and Gutzler 1981) in the surface temperature field were found in our 15-year run of the CCM0. Even when the control point was near the equator, the correlations were strongly damped but exhibited a noticable departure from isotropy as illustrated in Fig. 4. Apparently, the radiative coupling is very effective in damping any long-range interactions in the surface temperature field. Of course, this could reflect shortcomings in the GCM or in the peculiar symmetric boundary conditions that we have chosen to impose. This is not likely to be the case in upper air fields where long waves might be excited and not necessarily damped so efficiently.

Next, both the low-frequency and contemporaneous spatial spectra of the temperature fluctuations are presented in Fig. 5 based upon the 15-year undisturbed run. We have used the spherical harmonic basis for the representation of the spatial variance spectra. (Strictly speaking, one should exercise caution in using this representation for fields that have nonrotationally invariant statistics. It is akin to using Fourier periodo-

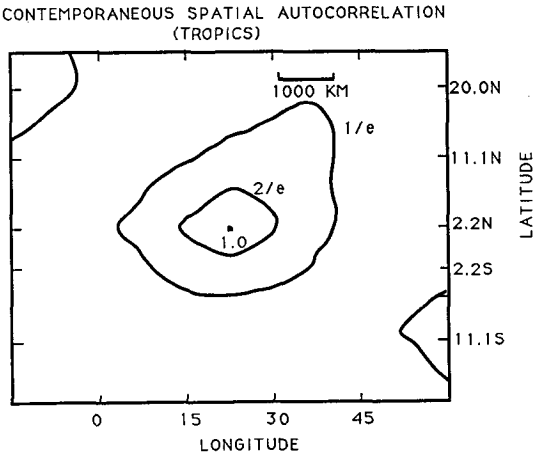

FIG. 4. Same as Fig. 1, except that the control point is near the equator (actually 2.2°N).

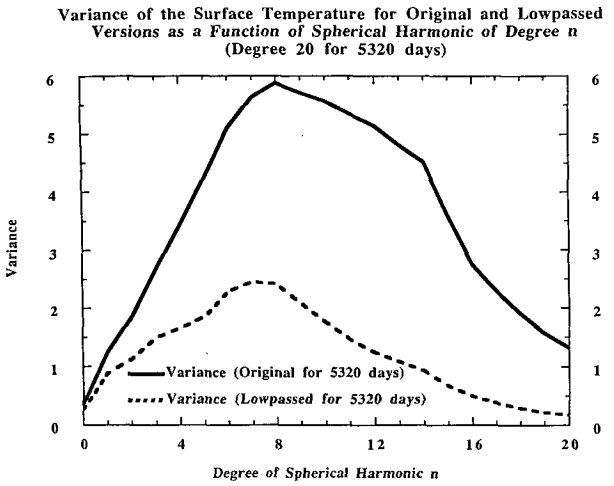

FIG. 5. Contemporaneous spatial spectrum by spherical harmonic degree n. Note that spatially white noise would lead to a linear graph (proportional to $2n + 1$, the number of zonal modes for each degree index). Hence, the spectrum corresponds to spatially white noise up to about degree 8, then the spectrum reddens. The discontinuous slope at degree 15 is due to the rhomboidal (R15) truncation in the CCM0 (cf. Fig. 6).

grams for nonstationary time series.) Recall that each spherical harmonic degree n has $2n + 1$ longitudinal modes, and hence a field that has equal variance in each mode ("equipartitioning" in statistical mechanics or "white spatial noise" in statistics) will have a spectrum that rises in proportion to $2n + 1$. This is illustrated schematically in Fig. 6 for the triangular truncation example. We see that the surface temperature fluctuations are essentially white up to degree 8 or 9 and then begin to "redden." It is the turning over at degree 8 or 9 that leads to a finite autocorrelation length on the sphere. (Recall that the autocorrelation function can be computed by a spherical harmonic transform of the spatial spectrum.) The sudden break in slope of the degree spectrum at $n = 15$ is due to the rhomboidal truncation in the CCM0. Essentially, there are less than $2n + 1$ modes per degree above $n = 15$ in the model, hence the "missing" power. The alternative truncation conventions are illustrated in Fig. 6 for the examples T5 and R5. The low-frequency limit spectrum illustrates to what extent the variance in smaller spatial scales is effectively removed by a very low-pass filter. As expected, most of the variance removed is in the higher degrees (smaller spatial scales).

Finally, we show some examples of temporal spectra for large spatial scales. The log of the smoothed spectral density (temporal) of the globally averaged temperature appears in Fig. 7 for the 15-year run (4096 days). On the same graph for illustrative purposes is the smoothed spectral density for a 512-day subset to give a rough indication of the sampling errors to be expected in such a shorter run. Also shown is the theoretical spectral density for an AR1 process (autoregressive process of order one; Newton 1988; Bendat and Piersol 1986) with autocorrelation time 30 days. Shown also in the figure are the bandwidth of the smoothing and the 90% confidence interval for sampling errors in both runs. The reason for the AR1 comparison is that simple EBMs forced by noise processes are expected to have solutions that exhibit AR1 behavior for each spherical harmonic mode amplitude (North and Cahalan 1981; Leung and North 1990, 1991). Although the fit does depart somewhat from AR1, it is a useful working model for what follows. Figure 8 shows the spectra for spherical harmonic amplitudes for index 40 (upper), index 20 (middle), and global-average index 00 (lower). Also shown on the graphs are the AR1 best fit models for these spectra. Again, we find reasonable agreement with the simple AR1 model as would be expected from the EBM studies.

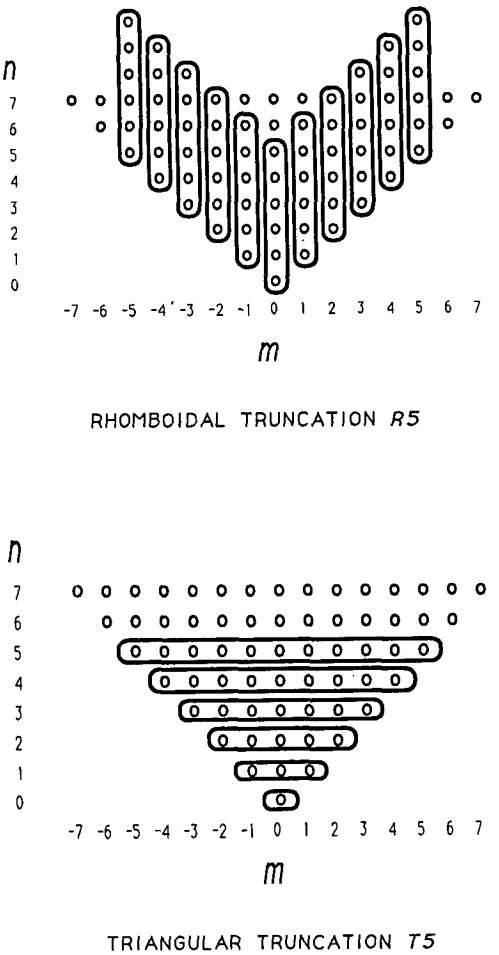

FIG. 6. Diagram showing the types of truncation for spherical harmonics $Y_{nm}(\hat{\mathbf{r}})$ commonly used in climate modeling. The upper diagram shows rhomboidal truncation R5 ($\sum_{m=-J}^{J} \sum_{n=|m|}^{|m|+J}$) and the lower shows triangular truncation T5 ($\sum_{n=0}^{J} \sum_{m=-n}^{n}$). The terms enclosed in loops are to be summed first, then the loops are to be summed in each type of truncation.

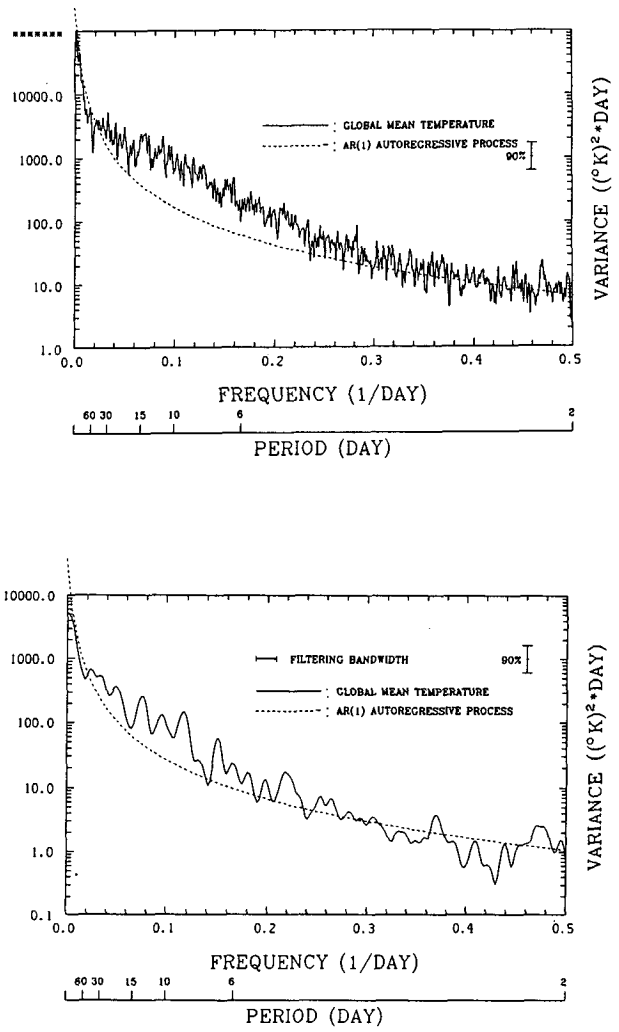

FIG. 7. Upper: log of the smoothed spectral density for the globally averaged surface temperature for a 4096-day run of the undisturbed climate. The dashed line is the theoretical curve for an AR1 process with autocorrelation time 30 days. The smoothing bandwidth is too narrow to be shown but is obvious from the texture of the graph; the corresponding sampling (90% confidence) interval is shown schematically for this length of time series. Lower: same except for a 512-day time series.

3. Response to perturbations

In this section, the response of the surface temperature field to externally applied forcing is considered. We choose two types of forcing for our experiments. First, temporally periodic forcing of the large-scale field is examined. We look to see if the response of the system is linear in its largest spatial scales and if higher harmonics of the forcing appear in the responses. Second, the response to point and line sources of heat located at the surface of the planet is examined. This gives us some idea about how faithful EBMs, for example, might be expected to imitate the response to surface perturbations such as albedo changes. In particular, we want to know about the linearity of the response to these small-scale perturbations.

a. Variable solar input

Consider periodic sinusoidal variations of the solar parameter. This type of forced climate response has been considered in earlier studies of EBMs (North et al. 1983b, 1984) for frequencies of 10, 1 and 0.1 yr^{-1}. In those studies, the goal was to understand the geographic patterns of the response when the planet has its current land–sea distribution. The reason for this choice of frequencies was because the atmosphere over land has a relaxation time of about 0.1 yr and the mixed layer of the ocean has a relaxation time of about 5 years. In the present applications, we look only at frequencies greater than 1/(30 days) since that corresponds to the longest natural time scale in the all-land *Terra Blanda* model.

First we consider a large (20%) periodic variation of the solar parameter with a period of 30 days. Note that the 30-day period is about the $1/e$ autocorrelation point for the global average temperature, and this is only a fraction (actually only about 16%) of the full response that the model would exhibit in going from one steady state to another with solar constant 20% different (cf., e.g., North et al. 1983b). Figure 9 shows a time series of length 1360 days. The sinusoidal variation in the lower graph (global average temperature = T_{00}) is obvious. The upper curve is for the second-degree spherical harmonic amplitude of the temperature field T_{20}. It is essentially a measure of the equator-to-pole temperature difference, and it is forced by changes in the solar flux because of the latitudinal gradient of the solar flux at the top of the atmosphere. The periodic responses in T_{00}, T_{20}, and even in T_{40} are clearly significant (outside the 90% error bars) as shown in their log spectra in Fig. 10. For comparison, we show smoothed spectral densities on a linear scale in Fig. 11. The latter gives some idea how much of the variance is contained in the forced-frequency bands compared to the continuum. One very important feature of these spectra is the absence of significant harmonic peaks. Low-order harmonics do not appear to be excited by the pure tone forcing at these weak amplitudes. That the higher modes behave in a linear manner similar to T_{00} is very important, since the nonlinearity might be argued to be felt mostly in the higher modes. This is so because the strength of the large-scale heat fluxes bears directly on the pole-to-equator temperature profile, whereas the fluctuations in horizontal heat fluxes is integrated out in a global average.

Figure 12 shows the response to a 40% sinusoidal variation of the solar constant at 30-day period. For further comparison, Fig. 13 shows the 40% amplitude forcing at a period of 60 days. At this strength of forcing we begin to see significant harmonics at 1/(15 days) and 1/(10 days). While apparent in the sense of detecting these harmonics, they constitute very little of the variance compared to the fundamental (<1%).

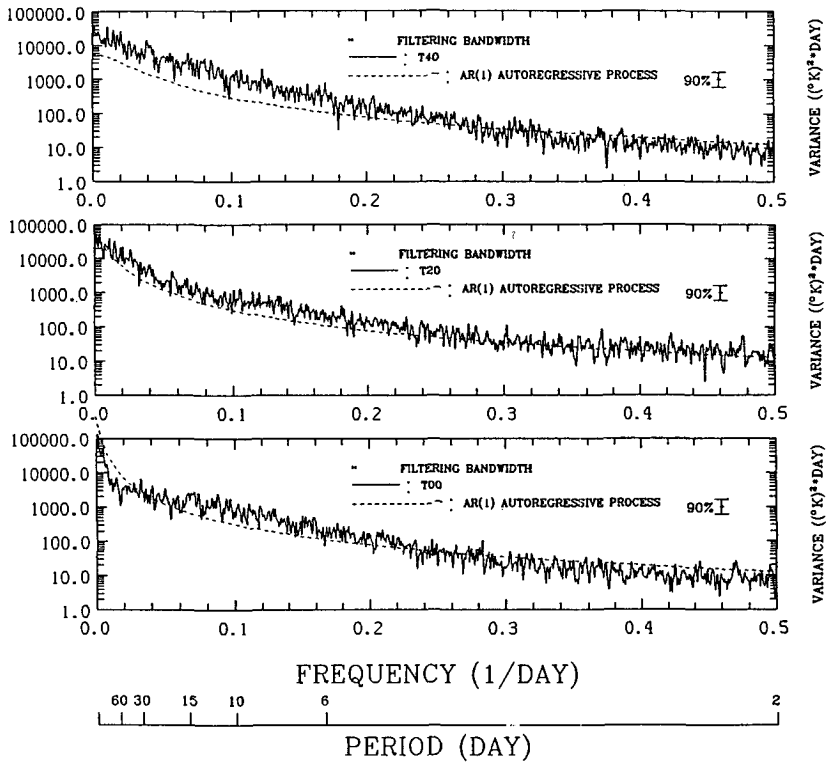

FIG. 8. Log of spectral density for time series of length 4096 days for (a) the global averaged mode, (b) the second Legendre polynomial amplitude, and (c) the fourth Legendre polynomial amplitude.

Another series of experiments were conducted at solar flux harmonic amplitudes of 10% and 5%. We found that the amplitude of the periodic response scaled linearly with the amplitude of the periodic forcing, as shown in Fig. 14. Also, the peak in the spectrum grew as the length of the time series was increased, indicative of a system with a continuous spectrum with a deterministic (in the statistical sense) sinusoid added (cf. MacDonald 1989). This is reasonable since contributions at frequencies away from the forcing will have random amplitudes and will tend to cancel as the series is lengthened, leaving a growth as only the square root of the length of the series; whereas a deterministic signal will not have random amplitudes or phases and will grow as the length of the series. The normalization convention of the spectral density will cause the deterministic line in the spectrum to grow relative to the continuum portions as the square root of the time series length. Experiments run with sinusoidal forcings of period 15 days were consistent with the above findings. In another experiment, a period of 60 days was used with the forcing at a strength of 20%, since the response at the lower frequency is much larger and presumably constitutes a cleaner test of linearity. The amplitudes of harmonics at 1/(30 days) and 1/(20 days) were much smaller (not significant) than those shown in Fig. 12.

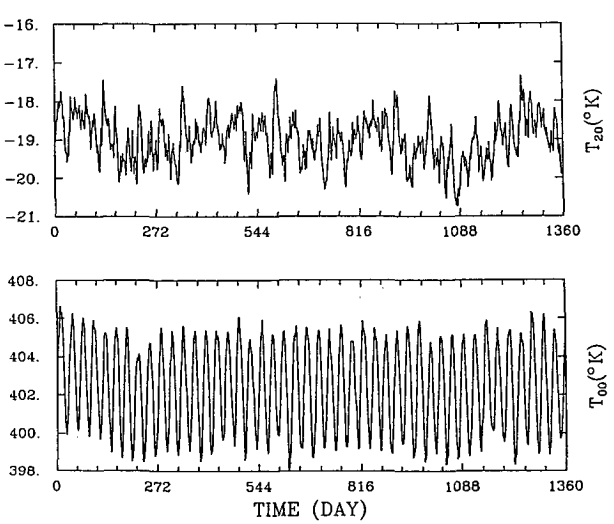

FIG. 9. Time series for two temperature modes when the system is forced by a sinusoidal (period 30 days) 20% perturbation to the solar constant. The upper curve is the second Legendre mode amplitude, and the lower curve is for the globally averaged temperature.

Finally, we can report results of an unrelated study (Bell 1991) in which the solar constant was abruptly changed by ±4%. The asymptotic response to the two shifts was symmetric with $|\Delta\bar{T}| \approx 4.5°$.

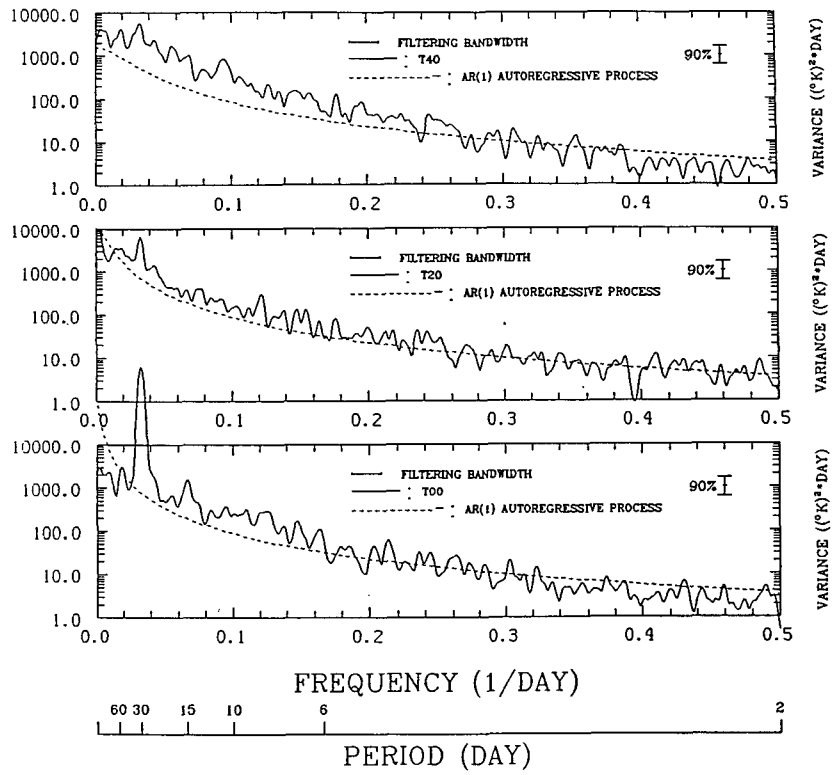

FIG. 10. Logarithms of smoothed spectral densities for the Legendre modes, T_{40} (upper), T_{20} (middle), and T_{00} (lower) for a 20% amplitude sinusoidal variation in the solar constant with period 30 days. Note that all have significant peaks at the 30-day period but not at the harmonics of this frequency. Plotted for reference as dashed lines are AR1 spectra with appropriate time scales.

b. *Steady surface heat sources*

In the last section, experiments on large spatial scales at specific frequencies of forcing were discussed. In this section we consider the effects of a point heat source located at the planetary surface. This is the kind of perturbation that might, for example, be expected from a patch of ice or some other perturbation in the surface albedo. Figure 15 shows the distribution of ensemble-averaged thermal response to a point heat source of 400 W m^{-2} located at 60° latitude. This strength of forcing was chosen since it is comparable to the solar forcing and also comparable to naturally occurring phenomena such as a strong precipitation feature. Computation of the average response was difficult since the standard deviation of temperature fluctuations at this latitude is about 15° and the response at the point in question is only about 4°. This meant either a very long run or taking some advantages of the symmetry of the planet. We chose to place four point sources equally spaced around the longitude belt at 60° latitude in each hemisphere. This strategy would fail of course if the "picket fence" heat source excited a standing wave in the field; this did not seem to be the case. The results shown in Fig. 15 are from using the picket fence heat sources in a run of 400 model days and pooling the data from all eight sectors. Note first the degree of isotropy present in the influence function contour map. The small displacement eastwards can be attributed to the same source (advection) as discussed earlier in connection with temporally lagged spatial correlations. The advection contribution is, of course, very small compared to the diffusive component. Note that the length scale is similar to that for simultaneous autocorrelations in the same but undisturbed model. There is a comparable lengthening of the length scale on the northern side of the heat source. This would increase the gradient on that side and possibly increase the size of D on that side if D were an increasing function of $|\nabla T|$ (we thank P. Stone for pointing out this possibility, personal communication 1991).

We have conducted the same experiment with a different strength of forcing (5/8 as much) and found that the shape of the ensemble-average influence function was identical except for the linear (5/8) scaling. An equal strength negative point heat source was also conducted with the now-expected linear response. (Experiments with surface heat sources in the tropics led to similar results with no midlatitude teleconnections apparent.)

Finally, we consider a band of surface heating located at 60° latitude, 3 grid points wide (approximately 15°

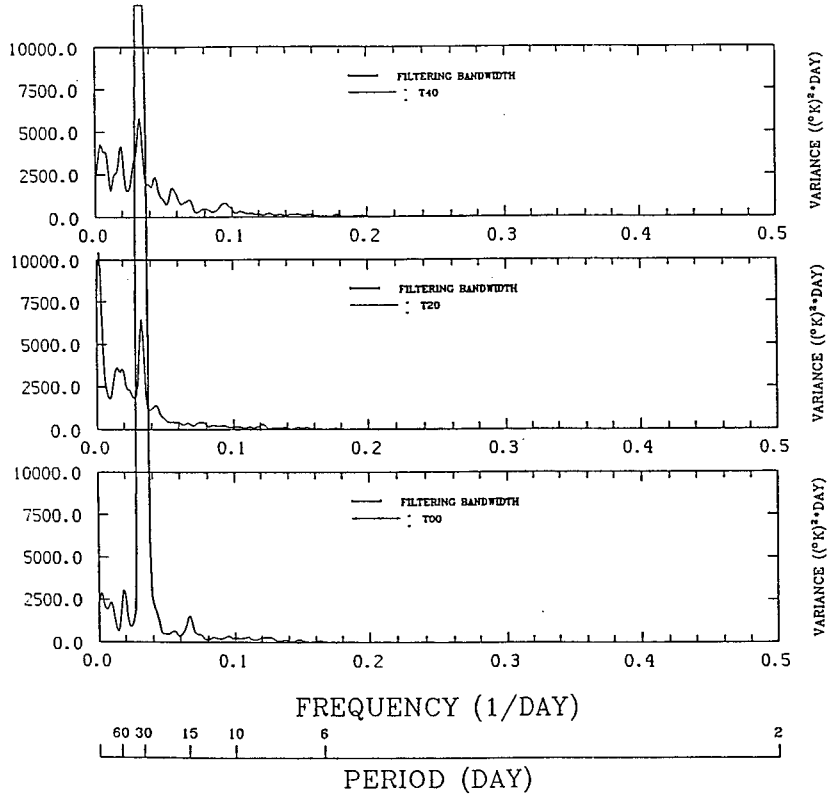

FIG. 11. Same as Fig. 10, except that the smoothed spectral density is shown on a linear vertical scale. This type of spectral plot has the advantage that equal areas under the curve represent equal contributions to the total variance in contrast to the log case, which is more convenient for showing statistical significance.

of latitude), and extending around the whole latitude circle. A complementary heating band is located in the opposite hemisphere to increase sampling statistics. The equivalent heat rate density is 50 W m^{-2}. The finite width band was chosen to remove any possible confusion about singularity of point or line sources. This latter is a concern for us since the EBM Green's function is singular (but integrable) at the source [it is a $K_0(s/l)$ (s is distance from the source, l is the length scale alluded to earlier; see North 1984) Bessel function] and this makes it difficult to compare with the GCM result. The ring-of-heat Green's function is also readily computed for the EBM and is given by (North et al. 1981)

$$\Delta T = g \sum_{n=0,2,\ldots}^{N} \frac{(2n+1)P_n(\sin(\theta_s))P_n(\sin(\theta))}{n(n+1)D + B}, \quad (1)$$

where θ_s is the latitude of the source; θ is the latitude of the point being examined; $P_n(\sin(\theta))$ is the nth Legendre polynomial; N is a truncation level (rhomboidal = triangular for zonally symmetric functions); D is the thermal diffusion coefficient, typically about 0.2 (earth radii)$^{-2}$W(°C)$^{-1}$; B is the radiation damping coefficient, typically about 2.0 W (m^2 °C)$^{-1}$; and the climate length scale is $l \sim \sqrt{D/B}$ in earth radii. The strength of the heat ring, g, is such that it is equivalent to the 15° band with 50 W m^{-2} used in the GCM.

The GCM result is shown in Fig. 16 for both hemispheres. Note that a curious warming is found at the poles. We believe this behavior of the CCM0 is spurious and due to truncation at R15. This is hinted at by the partial sums of the EBM formula above and shown in Fig. 16 for $N = 15$ and $N = 30$. Note that the EBM partial sum truncated at $N = 15$ also shows the spurious warming at the pole, but that it disappears at the higher truncation level. While this hardly constitutes a proof that the GCM is producing spurious truncation errors at the poles, it suggests that any results sensitive to polar thermal fields calculated by R15 climate models might be less securely based than previously thought.

A second CCM0 run was conducted with the band of heat but at half strength. The zonally averaged response is shown in Fig. 17. This curve shows more sampling error (weaker signal but same noise), as is evident by its slight lack of cross-hemispheric symmetry. The response scales by 50% rather exactly except for the anomalous polar behavior alluded to above.

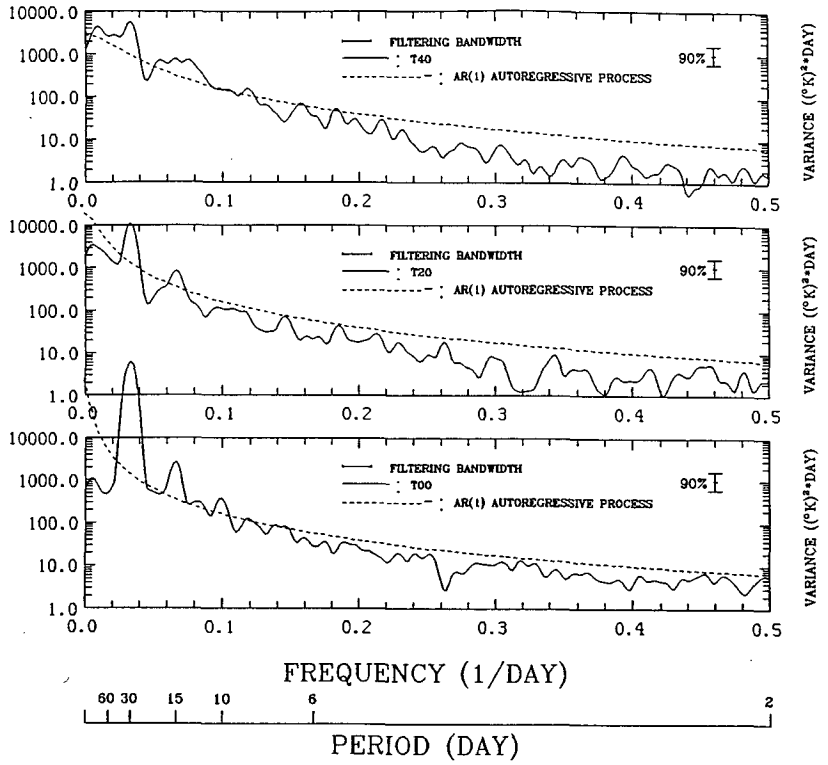

FIG. 12. Same as Fig. 10, except the amplitude of the forcing is 40%. Note the appearance of harmonics at 1/(15 days) and 1/(10 days).

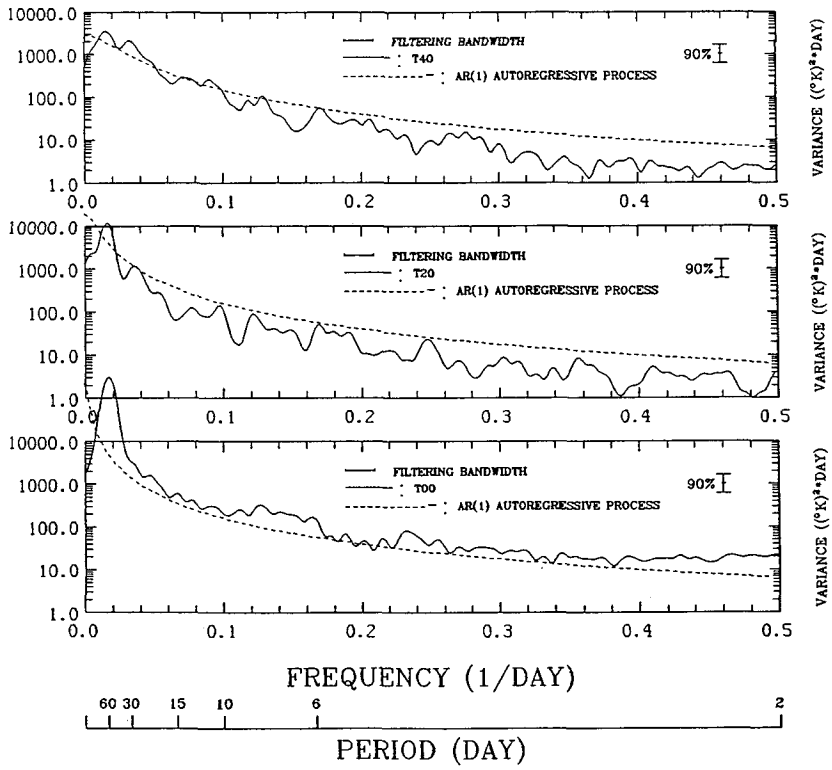

FIG. 13. Same as Fig. 10, except the period of forcing is 60 days.

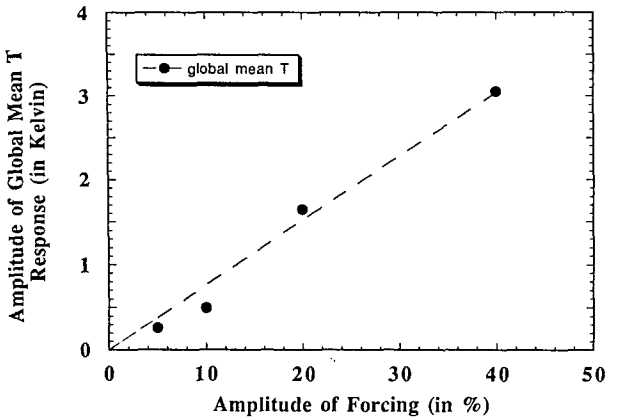

FIG. 14. Amplitude of response versus amplitude of sinusoidal forcing at period 30 days. The dashed line is a least squares fit to the four points passing through the origin.

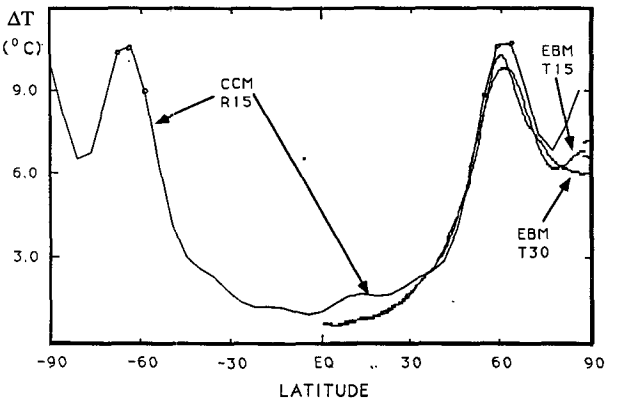

FIG. 16. Influence function for a 15° wide band of heat centered at 60° in each hemisphere. The curve shown for both hemispheres is from the CCM0 as indicated with a heating density of 50 W m^{-2} in the band. In the rightmost hemisphere are shown two Green's functions calculated from Eq. (1) for an EBM truncated at degree 15 and degree 30. Note the likely spurious warm anomaly at both poles in the CCM0 and in the truncated EBM.

4. Climate predictability of the second kind

It is interesting to speculate on what our results imply about the predictability of climatic moments under changes in external forcing. Consider the undisturbed runs. One issue concerns the finiteness of the variance of the large-scale temperature field at low frequencies. For example, we can ask about a time average

$$\bar{T}(t) \equiv \frac{1}{\tau}\int_{t-\tau/2}^{t+\tau/2} T(t')dt', \qquad (2)$$

where τ is the averaging interval. Now consider the variance of the time-averaged temperature, which can be expressed most conveniently in the Fourier representation

$$\mathrm{var}\bar{T} = \int_{-\infty}^{\infty}\left(\frac{\sin 2\pi\tau f}{2\pi\tau f}\right)^2 S_T(f)df, \qquad (3)$$

where $S_T(f)$ is the spectral density of T. Our concern is that the integral for $\mathrm{var}\bar{T}$ may diverge for a fixed τ especially at low frequencies (H. Levine and G. MacDonald take this approach in the CHAMMP report soon to be published, personal communication 1990). This might be the case in certain chaotic systems, for example. That the spectrum in our case appear to be finite in the limit of low frequencies suggests that the system is well behaved and has a well-defined

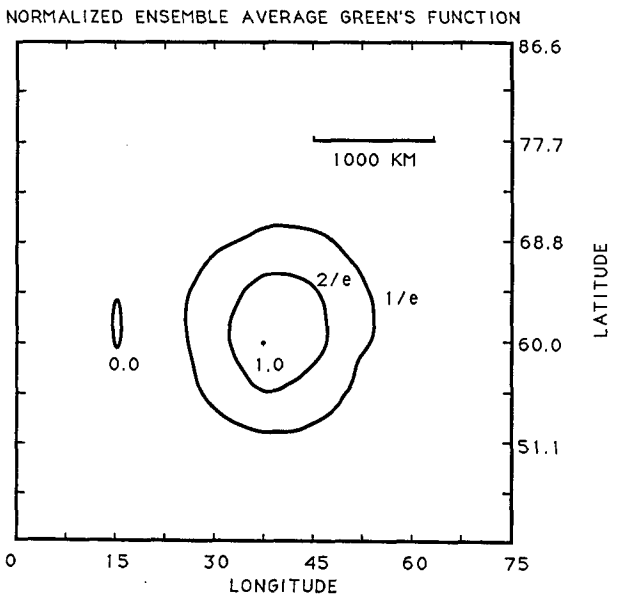

FIG. 15. Ensemble-average influence function for a point heat source at the surface of strength 400 W m^{-2}.

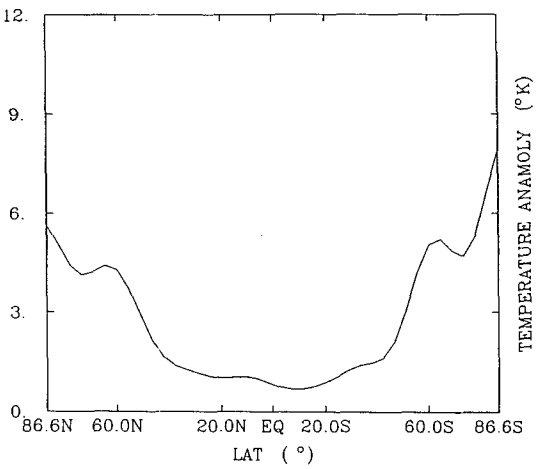

FIG. 17. Same as in Fig. 15, except that the strength of the heat source is 25 W m^{-2}. Lack of reflection symmetry between the hemispheres is due to sampling error. Note that the polar warming anomaly is even more strong (relative to the heat source) in this case.

mean and a finite variance over a band of low frequencies covering the lower limit. This means that long runs with fixed boundary conditions will lead to consistent estimates of the climatic means under control and altered conditions. Of course, we run into the classic problem of how long is long enough in our spectral estimation. We are looking at empirical (albeit computer generated) data here, and our conclusion seems to hold in runs of up to 180 autocorrelation times, which would be equivalent to nearly 1000 years of a model with a mixed-layer ocean.

5. Conclusions

The CCM0 experiments described above suggest that in the presence of highly symmetric surface boundary features and perpetual equinox solar distribution, there exists a linear response of the ensemble-averaged surface temperature field to large spatial-scale temporally periodic forcing of the heat balance in the model and to steady point and band heat sources at the planetary surface in high latitudes. These findings suggest that use of a linear Green's function is justified in simplified model studies (e.g., Salmun et al. 1978; Cahalan and North 1979; North et al. 1981; North 1984). Surface temperature data from the CCM0 appear to be representable by a simple linear radiation-damped diffusive EBM with blue spatial-noise forcing (peaking at spherical harmonic degree around 13, then reddening) and white temporal-noise forcing. A climate and radiation length scale l emerges in the CCM0 data that appears to be the one found in actual surface station data and calculable in the EBMs in terms of the diffusive and radiation parameters. The same length scale in the CCM0 or the noise-forced EBM comes from the studies of correlation of natural fluctuations or from the Green's function for steady heat sources. It is further encouraging that the value of the diffusion parameter found in the present studies is in reasonable agreement with the one found in fitting the EBM to the earth's seasonal cycle.

We list here some implications of our results.

1) The apparent cancellation of higher harmonics of forcing frequencies in the ensemble average suggests that surface (thermal) climate (in low-order GCMs) is determined by essentially linear heat transfer operators. This may mean that the possibility of modeling future climates with GCMs is easier (more robust) than previously thought.

2) The finite horizontal surface length scale ($l \sim$ 1000–2000 km) emerging in this study may mean that the coarse resolution models of the present may give reasonable results for the surface temperature climate. That is to say, details inside of such a circle are so highly correlated that no essential new thermal information is contained in them. This, of course, needs further testing.

3) The spectral distinction of forced (line spectra with no harmonics) and free variations (spectral continua) in this study is reminiscent of the similar apportionment of variance introduced and referred to as "forced" and "free" variations by Lorenz (1979). We think this "clean" apportionment holds especially well for the surface temperature field. In our view, forced means that a peak in a band in the spectrum grows relative to the continuum as the time series is lengthened proportional to the square root of the time series length, whereas a free variation leads to a peak that converges to a finite value in a band.

4) With the foregoing findings it should be possible to reintroduce the *trivial* (compared to Navier-Stokes advection-type) or macro-nonlinearities, such as snow–ice feedbacks, with less difficulty than we might have thought earlier. This, of course, does not mean that these quantities (i.e., sea ice) are necessarily easy to calculate.

5) The results found here renew the hope that independent checks on climate sensitivity may be revealed in studies of present-day climate statistics such as the autocorrelation parameters. This is reminiscent of the so-called Fluctuation Dissipation Theorem (FDT) possibilities discussed by Leith (1975), Bell (1980), and North et al. (1981). If the basic atmospheric climate is linear as suggested here, the FDT is satisfied trivially. In particular, in the present homogeneous-planet case the sensitivity is proportional to the autocorrelation times for individual temperature modes independently. The extension of our work to a heterogeneous planet (land and ocean surfaces) where several time scales are present is clearly of interest.

6) The results found here and in Leung and North (1991) concerning the contemporaneous spatial spectrum and for low frequencies imply that at least in this model the variances contained in finite spherical harmonic degree bands are *bounded,* and therefore some degree of predictability of the second kind will exist for all spatial scales in atmosphere-only models of this type. Of course, the same and much more difficult question for the ocean–atmosphere coupled system naturally arises. This is one of the key questions that must be addressed by the modeling community in the next decade.

All of the above conclusions (conjectures really) are model dependent. Many additional experiments need to be conducted in order to further test the possibilities advanced here based upon the CCM0-*Terra Blanda* studies. First, the CCM0 is far simpler than nature. We can easily repeat some of our experiments with more advanced versions of the CCM such as CCM1 or other contemporary models. We intend to proceed along these lines next. Second, we need to find out if some of our simplifications, such as no mountains, are significant to our main conclusions. Eventually, we need to test the importance of the land–sea (and other) sources of heterogeneity on our climate system.

Acknowledgments. We are grateful to several sources for their support. The National Science Foundation's Climate Dynamics Program provided a research grant. Some graduate student support came from the Texas A&M Office of University Research. The computing was supported partially by a grant from Cray Research and partially by funds from a Department of Energy grant. One of us (L.-Y. L) has also been partially supported by a grant administered by Washington State University for Batelle Pacific Northwest Laboratories. The National Center for Atmospheric Research is supported by the National Science Foundation. One of us (GRN) also wishes to acknowledge the friends (too many to list) who listened patiently to his long expositions of this work. Many helpful suggestions came from these interactions.

REFERENCES

Bell, R., 1991: Fluctuation–dissipation relation in climate theory. M.S. thesis, Department of Physics, Texas A&M University, 50 pp.

Bell, T. L., 1980: Climatic sensitivity and fluctuation–dissipation: Some simple model tests. *J. Atmos. Sci.,* **37,** 1700–1707.

Bendat, J. S., and A. G. Piersol, 1986: *Random Data, Analysis and Measurement Procedures,* second ed. Wiley-Interscience, 566 pp.

Cahalan, R. F., and G. R. North, 1979: A stability theorem for energy-balance climate models. *J. Atmos. Sci.,* **36,** 1205–1216.

——, D. A. Short, and G. R. North, 1982: Cloud fluctuation statistics. *Mon. Wea. Rev.,* **110,** 26–43.

Chervin, R. M., 1986: Interannual variability and seasonal climate predictability. *J. Atmos. Sci.,* **43,** 233–251.

Hoerling, M. P., T. K. Schaack, and D. R. Johnson, 1990: Heating distributions for January and July simulations of the NCAR Community Climate Model. *J. Climate,* **3,** 417–434.

Hyde, W. T., K.-Y. Kim, T. Crowley, and G. R. North, 1989: A comparison of GCM and energy balance model simulations of seasonal temperature changes over the past 18 000 years. *J. Climate,* **2,** 864–887.

Kim, K.-Y., and G. R. North, 1991: Surface temperature fluctuations in a stochastic climate model. *J. Geophys. Res.,* submitted.

Leith, C. E., 1975: Climate response and fluctuation dissipation. *J. Atmos. Sci.,* **32,** 2022–2026.

Leung, L.-Y., and G. R. North, 1990: Information theory and climate prediction. *J. Climate,* **3,** 5–14.

——, and ——, 1991: Atmospheric variability on a zonally symmetric land planet. *J. Climate,* in press.

Lorenz, E. N., 1979: Forced and free variations in weather and climate. *J. Atmos. Sci.,* **36,** 1367–1376.

MacDonald, G., 1989: Spectral analysis of time series generated by nonlinear processes, *Rev. Geophys.* **4,** 449–470.

Malone, R. C., E. J. Pitcher, M. L. Blackmon, K. Puri, and W. Bourke, 1984: The simulation of stationary and transient geopotential-height eddies in January and July with a Spectral General Circulation Model. *J. Atmos. Sci.,* **41,** 1394–1419.

Newton, H. J., 1988: *Timeslab: A Time Series Analysis Laboratory.* Wadsworth & Brooks/Cole, 623 pp.

North, G. R., 1984: The small ice cap instability in diffusive climate models. *J. Atmos. Sci.,* **41,** 3390–3395.

——, and J. A. Coakley, 1979: Differences between seasonal and median annual energy balance model calculations of climate and climate sensitivity. *J. Atmos. Sci.,* **36,** 1189–1204.

——, and R. F. Cahalan, 1981: Predictability in a solvable stochastic climate model. *J. Atmos. Sci.,* **38,** 504–513.

——, J. A. Coakley, and R. F. Cahalan, 1981: Energy balance climate models. *Rev. Geophys. Space Phys.,* **19,** 91–121.

——, J. G. Mengel, and D. A. Short, 1983a: Simple energy balance model resolving the seasons and the continents: Application to the astronomical theory of the ice ages. *J. Geophys. Res.* **88,** 6576–6586.

——, ——, and ——, 1983b: *Climatic Response to a Time Varying Solar Constant. in Weather and Climate Responses to Solar Variations.* B. M. MacCormac, Ed., Colorado Associated University Press, 243–256.

——, ——, and ——, 1984: On the transient response patterns of climate to time dependent concentrations of atmospheric CO_2. *Climate Processes and Climate Sensitivity, Geophys. Monogr.* **29,** Amer. Geophys. Union, 164–170.

Pitcher, E. J., R. C. Malone, V. Ramanathan, M. L. Blackmon, K. Puri, and W. Bourke, 1983: January and July simulations with a Spectral General Circulation Model. *J. Atmos. Sci.,* **40,** 580–604.

Ramanathan, V., E. J. Pitcher, R. C. Malone, and M. L. Blackmon, 1983: The response of a spectral general circulation model to refinements in radiative processes. *J. Atmos. Sci.,* **40,** 605–630.

Randel, W. J., and D. L. Williamson, 1990: A comparison of the climate simulated by the NCAR Community Climate Model (CCM1:R15) and ECMWF analyses. *J. Climate,* **3,** 608–633.

Salmun, H., R. F. Cahalan, and G. R. North, 1980: Latitude-dependent sensitivity to stationary perturbations in simple climate models. *J. Atmos. Sci.,* **37,** 1874–1879.

Saltzman, B., 1978: A survey of statistical–dynamical models of the terrestrial climate. *Advances in Geophysics,* Vol. 20, Academic Press, 183–304.

Stone, P., 1978: Baroclinic adjustment. *J. Atmos. Sci.,* **35,** 561–571.

Wallace, J. M., and D. S. Gutzler, 1981: Teleconnections in the geopotential height field during the Northern Hemisphere winter. *Mon. Wea. Rev.,* **109,** 784–812.

Washington, W. M., (Ed.), 1982: *Documentation for the Community Climate Model* (CCM), Version 0. National Center for Atmospheric Research, [NTIS No. PB82-194192].